Optical characteristics of type-II hexagonal shaped GaSb Quantum dots on GaAs synthesized using nanowire self-growth mechanism from Ga metal droplet

Min Baik
Yonsei University
Ji-hoon Kyhm
Dongguk University
Hang-Kyu Kang
Yonsei University
Kwang-Sik Jeong
Yonsei University
Jong Su Kim
Yeungnam University
Mann– Ho Cho
Yonsei University
Jin Dong Song (jdsong72@gmail.com)
Korea Institute of Science and Technology

Research Article

Keywords: transmission electron microscope (TEM), quantum dots

Posted Date: February 17th, 2021

DOI: https://doi.org/10.21203/rs.3.rs-200110/v1

Version of Record: A version of this preprint was published at Scientific Reports on April 8th, 2021. See the published version at https://doi.org/10.1038/s41598-021-87321-9.

Abstract

We report the growth mechanism and optical characteristics of type-II band-aligned GaSb quantum dots (QDs) grown on GaAs using droplet epitaxy-driven nanowire formation mechanism in with molecular beam epitaxy (MBE). Using transmission electron microscope (TEM) and scanning electron microscope (SEM) images, we confirmed that the QDs, which comprise zinc-blende crystal structures with hexagonal shape, were successfully grown through the formation of a nanowire from a Ga droplet with less strain between GaAs and GaSb. Photoluminescence (PL) peaks of GaSb, which are capped by the GaAs layer, are observed at 1.11 eV, 1.26 eV, and 1.47 eV, assigned to the QDs, a wetting-like layer (WLL), and bulk GaAs, respectively, at the measurement temperature of 14 K and excitation laser power of 30 mW. The integrated PL intensity of the QDs is significantly stronger than the WLL, which indicates well-grown GaSb QDs on GaAs and the generation of an interlayer exciton, as shown in the power and temperature-dependent PL, respectively. In addition, Time-resolved PL (TRPL) data show that the GaSb QD and GaAs layer form a self-aligned type-II band alignment, and temperature-dependent PL data exhibit a high equivalent internal quantum efficiency of 15+/-0.2%.

I. Introduction

Group III–V materials with direct bandgaps are actively studied as novel materials in photonics because it is possible to control the electrical and optical characteristics according to the structure and dimensions.[1–4] In particular, many researchers have studied Sb-based III-V materials for wide range of application as a next generation in the telecommunication society [1]. Furthermore, the charge separation in the materials is significantly dependent on the type of band alignment because differences in band alignment lead to changes in several physical quantities, such as the recombination rate and emission wavelength. Due to this clear dependence, the optically modulated characteristics resulting from the band alignment are continuously researched on 3-dimensional bulk systems, as well as on 1-dimensional nanowires or 0-dimensional quantum dots (QDs). Considering the dimension and size of the materials, a QD is a perfect system for analyzing zero-dimensional quantum effects.

In this study, we synthesized a GaSb QD on a GaAs substrate using a self-grown method by droplet epitaxy[5] with a molecular beam epitaxy (MBE) system.[2,3] We investigated the optical properties of the QD, which are dependent on its type-II band alignment in the GaSb/GaAs hetero-structure, which is different from the type-I band structure of InAs/GaAs.[6–12] In detail, charge separation can occur more easily in the GaSb QD because the GaSb QD forms a type-II band alignment with GaAs. The structure of the GaSb QD shows that the QD has zinc-blende crystal structure with hexagonal shape. We characterized the well-grown GaSb QDs using power-dependent and temperature-dependent photoluminescence (PL). The peak shift to a higher energy clearly suggests a type-II band alignment. Furthermore, we cross checked that the GaSb QD and GaAs layer formed a type-II band alignment by time-resolved PL (TRPL) data. Considering the superior PL characteristics resulting from the type-II band alignment, the equivalent internal quantum efficiency (E-IQE) of the GaSb QD is ~ 15% by using the ratio of intensity between 300 K and 14 K. In

conclusion, GaSb QD was successfully grown through the nanowire self-growing mechanism on GaAs with a type-II band alignment, and a high equivalent internal quantum efficiency (IQE) was confirmed using temperature-dependent PL data.

Ii. Result And Discussions

The GaSb QD was grown on n-type GaAs(001) wafers using MBE systems. First, to reduce the native defects on the GaAs substrate, we grew sequentially a 200-nm-thick GaAs buffer, a short-period superlattice (SPS) structure with two alternate layers (5 nm-thick $Al_{0.3}Ga_{0.7}As$ and a 5-nm thick GaAs), and a 75-nm-thick GaAs layer at the growth temperature of 580°C.[13–15] Then, we cooled down the substrate to 350°C with valve of arsenic (As) cracker cell and main shutter (MS) open to prevent from vaporizing the As of buffer layer. the As After that, we closed the valve of As cracker cell and the MS because the GaAs substrate is thermally stable under 350°C, as shown in Figure S1.[16–18] Next, a gallium (Ga) droplet was formed on the top of the GaAs layer in an ultra-high vacuum of less than 1×10^{-9} Torr at 250°C for 10.6 s, as shown in Figure S2. The time was equivalent to the growth time of the 5-monolayer (ML) GaAs. After cooling the substrate to 180°C, the Antimony(Sb) dimer was supplied to the Ga droplets at 180°C for 5 min, resulting in the diffusion of Sb to the Ga droplets, as shown in Fig. 1(a). Thus, the GaSb QD was grown by supplying the Sb to the Ga droplets on the GaAs surface, as shown in Fig. 1(b). For the QD without a capping layer, the growth process was complete. A two-step process was used to prevent the QD from melting while the GaAs capping layer was being grown. First, the GaAs was grown on top of the surface at 280°C to prevent the GaSb QD from melting without growth stop. Next, the substrate temperature was increased to 500°C for the growth of an additional GaAs capping layer under an optimized condition. As a result, a ~ 17-nm-thick GaAs capping layer was grown. The main parameters of the growth condition, which consisted of the substrate temperature (Ts), beam equivalent flux (FAs), and growth time (t_g), were optimized, as shown in Figure S1.

To confirm the formation of the QD, we measured the structural and morphological characteristics of the sample without the GaAs capping layer using atomic force microscopy (AFM), scanning electron microscope (SEM), and transmission electron microscope (TEM). First, the surface morphology of the sample was analyzed using AFM to confirm the shape of the QD. The AFM data in Fig. 2(a) clearly present the morphological shape of the film surface containing the QD and the wetting-like layer (WLL), with the root mean square roughness (Rq) being ~ 3 nm. Second, SEM and TEM were used to confirm the shape, distribution density, and diameter of the QDs. From the SEM and TEM data shown in Fig. 2(b) and (c), an average diameter of 100 +/- 5 nm was obtained for the QD. Focusing on the zone axis at the [111] direction, it is found that the nanostructure of the GaSb QD is not spherical nor pyramidal-shape; rather, the QD had a nanowire-like pillar shape with zinc-blende structure. The density of the QDs was less than 10 per μm^2, as shown in Fig. 2(b) and (c). Furthermore, considering Fig. 2(c) and Figure S2, the GaSb nanostructure was formed via the self-catalyst nanowire formation mechanism,[5] rather than the SK-growth mechanism.[17–20] Specifically, the Ga droplet was formed during 10.6 s, which is the same as deposition time of the 5-ML GaAs, as shown in Figure S2. After that, a 40nm-thick Sb layer was deposited

on the GaAs surface, as shown in Figure S3. GaSb nanowire was grown under the growth condition of the diffusion-limited process for the Sb atom. Since the migration of Sb was slow at 180°C,[21] the amount of Sb diffused into the Ga droplet was not sufficient. In this case, the Ga droplet was used as a self-catalyst for the QD growth like as the nanowire growth. During the growth of the QDs, the WLL observed around the GaSb nanostructure is not attributed to the growth of the GaSb QD. Most of the Sb is considered to be vaporized during the increase in the substrate temperature up to 280°C, and the origin of the WLL is attributed to the intermixing of residual Sb into GaAs layer.

To investigate the nanostructure of the samples further, we analyzed the cross-section TEM images, as shown in Fig. 3(a); a clear difference was observed, i.e., the top and bottom areas of the image indicate the GaSb QD and the GaAs layer, respectively. Each red square from the bottom to the top shown in Fig. 3(a) were used for fast Fourier transform (FFT), which are related to Fig. 3(b) and (c), respectively. Using the FFT images in Fig. 3(b) and (c), the elongated direction of the QDs is not parallel to the [001] direction of the GaAs substrate. The cross-sectional image reveals that the QD grown along the [111] direction of the GaAs layer had a zinc-blende structure. Using the reciprocal lattice constants of the GaAs layer in each direction, which were 2.93 nm^{-1}, 2.96 nm^{-1}, and 3.41 nm^{-1} from the selected-area diffraction (SAD) pattern, the diffracted plane was indexed based on the reported data, as shown in Fig. 3(b).[22–24] Moreover, using the reciprocal lattice constants of GaSb in each direction, which were 2.60 nm^{-1}, 2.71 nm^{-1}, and 3.17 nm^{-1}, the diffracted plane was indexed, as shown in Fig. 3(c). Based on the reported lattice constants of (111), (11 − 1), and (002), we indexed the plane of the reciprocal lattice following the length of each direction, as shown in Fig. 3(c). Furthermore, comparing with reported lattice constant of GaSb,[25–26] we confirmed that difference of lattice constant in GaSb QD is ~ 1.8%. From this result, we suggest that due to the high lattice mismatch between GaAs and GaSb over 7%, growth direction of GaSb QD was changed to reduce the strain, resulting in the most stable growth of the QD with minimum interfacial strain. In this process, the strain was reduced by ~ 1.8% along the [111] direction. As a result, we can confirm that the QD is well grown along [111] direction of GaAs, and it has ~ 1.8% lattice strain. As a result, the GaSb QD was grown by nanowire formation mechanism with limited amount of group III material.

To investigate the band alignment between the GaSb QD and GaAs layer, we performed a PL measurement. Figure 4 (a) presents the PL spectra for a QD sample measured at 16 K by changing the laser power from 1 mW to 30 mW. Considering the peak separation using Gaussian fitting, the PL peak at 1.05 eV can be attributed to the GaSb QDs, where the full width at half maximum (FWHM) is approximately 258 meV. The energy of the PL peak emission is somewhat lower than the GaSb QDs.[27–30] Three peaks are observed at 1.47 eV, 1.24 eV, and 1.32 eV; the first peak is attributed to bulk GaAs, and the other two peaks are attributed to a $GaAs_xSb_{1-x}$ WLL. As the laser power density increases, the peak at 1.05 eV from the GaSb QDs is observed to blue-shift up to 1.13 eV. However, the blue shift of the other two peaks at 1.24 and 1.32 eV from $GaAs_xSb_{1-x}$ WLL is weakened, as shown in Fig. 4(b). The behavior of clear blue shift with an increasing laser power at 1.05 eV is caused by the QD structure, because the shift originates from the Coulomb interaction and QD state-filling of the holes due to the spatial separation of

holes in the GaSb QD and the attracted electrons confined in the nearby GaAs regions.[31–33] On the contrary to the behavior, the peak shifts at 1.24 eV and 1.32 eV show the different from the nature of QDs. In addition, to confirm the GaSb QD properties, we investigated temperature-dependent PL, as shown in Fig. 4(c). Some properties were related to the QD structure of the GaSb embedded in the WLL, as shown in Fig. 4(c) and (d). In detail, as the temperature increases, an interlayer exciton is generated by the activated phonon, due to the interaction of holes in the GaSb QD with electrons in the $GaAs_xSb_{1-x}$ WLL. This process is reflected in the energy shift of the interlayer exciton to a low energy, as shown in Fig. 4(c) and 4(d). Since the calculated exciton Bohr radius in previous reported papers, ~ 20 nm, is similar to the dimension of the GaSb QD, as shown in Fig. 2,[34] a weak quantum confinement effect was generated in the QD. This effect contributed to the increase in peak intensity associated with the GaSb QD at 300 K. In addition, under the contribution of the phonon to the interlayer exciton, the PL intensity of the GaAs substrate and GaSb WLL is reduced. These optical characteristics indicate that a type-II band alignment was well formed in the GaSb QD/GaAs hetero-structure.

To confirm the type-II band alignment of the GaSb QD/GaAs hetero-structure, we investigated the carrier transfer mechanism by performing TRPL measurements at 300 K. Figure 5(a) presents the decay profile of the PL at 1.29 eV (WLL) and 0.99 eV (QD). The decay curve at 0.99 eV indicates mono-exponential behavior, which can be ascribed to the typical type-II staggered band alignment of GaSb QDs, and the long decay time is attributed to the reduced spatial overlap between the electrons in the WLL and the holes in the QDs. In comparison with long decay time, the decay curve of 1.29 eV presents a two-step process composed of a faster initial and slower tail component, as shown in the fitting parameters in Table 1. The average decay times $< t >$ of the QDs were estimated as a linear sum of weighted multiple exponentials, where $A_{i=1,2,\ldots}$ refers to the weighting coefficient for each exponential, and $\tau_{i=1,2,\ldots}$ indicates the corresponding fitted decay characteristic times.[35] In our fittings, we used up to I = 2, which provides a reasonable fit for the measured values. The average decay time varied from 2.3 to 12.5 ns from the decay curves at the different peak position as shown in Fig. 5(b). From decay times, we can estimate the charge-transfer rate constant k_{ct} following equation:

$$k_{ct} = 1/t_{WLL} - 1/t_{Tran} \quad (1)$$

where t_{WLL} and t_{Tran} are the average emission lifetimes of the GaSb WLL and the charge transfer, respectively. For the charge-transfer dynamics between a delocalized continuum state and a localized state, e.g., between a 2D wetting layer and a 0D QD, the functional form of this many-state Marcus model is as follows:

$$k_{ct} = \int_{-\infty}^{+\infty} \frac{2\pi}{\hbar} \rho(E) |H(E)|^2 \frac{1}{\sqrt{4\pi\lambda k_B T}} exp\left(-\frac{(\lambda+\Delta G+E)^2}{4\lambda k_B T}\right) dE \quad (2)$$

where ρ(E), H(E), and ΔG indicate the density of the accepting state, the electronic coupling, and the energy difference between the donor and acceptor energy levels, respectively.[36-38] The density of the states, ρ(E), is obviously different between a WLL (3D) and a QD (0D). The electronic coupling, H(E), which depends on the physical overlap between the transferred electron in its initial and final states, can be independent of energy due to the physical structure. ΔG can be expressed as $\Delta G = E_{h(QD)}-E_{h(WLL)}$, where $E_{h(QD)}$ and $E_{h(WLL)}$ are the energies of the hole at the QD and WLL, respectively. Since the PL spectrum is strongly related to the hole energy of the WLL and QD in a type-II system, we takeΔG to be linear relation with energy. As shown in Figure 5(c), the charge-transfer rate linearly increases in overall range, while the slope in the QD region has changed drastically. This sudden change is originated from the transition of ρ(E) between the WLL and QD. As a result, we cross check that the GaSb QD is well grown on the GaAs substrate and GaSb QD has type-II band structure with GaAs.

Following the reported paper[39], the PL data at 14 K were fitted with four peaks to calculate the E-IQE of the GaSb QD, as shown in Figure 6(a) and (b); the peaks corresponding to GaSb QD, WLL1, WLL2, and GaAs. However, the PL data at 300 K, fitted with one or two peaks, indicate that non-radiative emission process is increasing at a high energy, indicating that the effective charge transfer to the GaSb QD. Finally,we can extract the 15+/-0.2% E-IQE using the ratio of the GaSb QD fitting area. In conclusion, the self-grown GaSb QD on GaAs with a well-defined structure has a high E-IQE. To confirm the relationship between E-IQE and the lattice strain, we calculated the total band structure depending on the lattice strain in GaSb, as shown in Figure S4 (a) and (b). Following the simulation data, the band gap of GaSb with a 1.8% strain along the [111] direction is smaller than that of GaSb without strain. To be specific, the valance band degeneracy is broken by the lattice strainand, and the band gap with a strain become smaller than that without the strain, as shown in Figure S4 (c) and (d); this is consistent with the red shift of the QD PL. In general, the reported results indicate that the maximum efficiency of a QD decreases within the Shockley–Queisser limit, i.e., the lattice strain reduces the efficiency.[40] However, since the lattice strain from the self-grown GaSb QD in this study was minimized, we optimized the efficiency by controlling the lattice strain. In this self-grown QD formation, where the interfacial strain is minimized by changing the growth direction, the self-aligned type-II band structure with an optimized strain can affect the QD size and the formation of an effective band structure; this results in an improved efficiency compared with that of samples with a higher strain reported other paperss.[41-42]

Iii. Conclusion

In summary, we investigated the growth mechanism of a type-II GaSb QD grown on GaAs using a self-grown nanowire process. During the growth, a Ga droplet formed on top of the GaAs layer, and a hexagonal shaped GaSb QD with a zinc-blende structure is grown like as nanowire growth mechanism through the diffusion of the Sb into the Ga droplet. Based on PL data, we confirmed the state-filling effect in the GaSb QD with the type-II band alignment. In addition, using TRPL fitting data, we obtained two types of decay time constant, related to nonradiative and radiative decay, which is also consistent with the type of band alignment. Moreover, the formation of GaSb QD with the type-II band alignment with

GaAs layer by using self-growth mechanism like as nanowire decreases the interfacial strain through the change in growth direction, resulting in increasing E-IQE up to 15%. This study suggests the possibility of self-grown GaSb QD like as nanowire, which can successfully improve optical characteristics of the GaSb QD. Thus, this result shows that the GaSb QD can be self- grown by using GaSb droplet on GaAs considering the band alignment. Furthermore, it is very useful synthesis method to optimize the efficiency of various optical devices. For example, GaSb QD grown in this study can be used as a near IR sensor by bandgap tuning using lattice strain.

Iv. Method

GaSb QDs were grown on n-type GaAs(001) substrates in a RIBER compact-21E MBE system equipped with cryogenic and ion getter pumps. The system was also equipped with RIBER VAC500 valved-cracker-cell and VEECO Sb valved cracker cell to supply the As tetramer and Sb dimer elements, respectively. Ga, which is a group-III metal source, was supplied through an effusion cell. The flux of the group-III material was fixed at a specific value during the growth process. Top-view images of the QD samples were obtained using SEM. To analyze the nanostructure, morphology, and thickness of the GaSb QD, GaAs buffer layer, and GaAs SPS layer, we used an FEI Tecnai F-20 HR-TEM at an accelerating voltage of 300 kV. SAD patterns were transformed using FFT to analyze the crystal structure well formed in the GaSb QD/GaAs heterostructure. To confirm the type-II band alignment of the GaSb QD/GaAs hetero-structure, a PL measurement was performed using a 532-nm DPSS laser (30 mW, CNI laser) and a monochromator (SP-2300, Princeton Instruments) with a closed-cycle refrigerator (RW-3, Leybold). To investigate the carrier-transfer mechanism, we measured the TRPL at 300 K using a TCSPC module (Picoquant, PH-300) with an 800-nm Ti:sapphire laser (80 MHz, Mai-tai, Spectra-physics) and NIR-PMT (Hamamatsu, H10330c-75). To predict the effect of strain on the GaSb QD, density functional theory (DFT) calculations were performed using the Vienna ab-initio simulation package (VASP). A 500-eV cut-off energy and 9 × 9 × 9 k-points were used for the DFT calculations to make the spacing of the k-points under 0.2 (1/ang) with the Perdew-Burke-Ernzerhof revised for solids (PBEsol) function. The GaSb unit cell was geometrically optimized until convergence with 0.005 eV/ang. To simulate the strain effect on the GaSb QD, 1.8% of the tensile strain in the [111] of the GaSb unit cell ([001] direction of the re-defined hexagonal cell) was applied, based on the measured strain in the TEM images. The lattice parameter in the other directions ([100] and [010] of the re-defined hexagonal like a cell) was relaxed until the stress in those direction was smaller than 0.01 GPa. During relaxation, a 500-eV cut-off energy and 9 × 9 × 3 k-points were used. To obtain an accurate band structure for the strained GaSb, we performed DFT calculations with the hybrid functional Heyd-Scuseria-Ernzerhof 06 (HSE 06). A 500-eV cut-off energy and 9 × 9 × 9 k-points were used for calculating the GaSb band structure.

Declarations

Corresponding Author

To whom correspondence should be addressed.

E-mail: mh.cho@yonsei.ac.kr & jd.song@kist.ac.kr

Author Contributions

Min Baik and Ji-hoon Kyhm contributed equally to this work.

M. Baik M-H Cho and J.D. Song designed the experiments and analyzed the data. J. Kyhm performed and analyzed optical characterization. K-S Jeong performed simulation for band structure of GaSb depend on strain. M. Baik, H-K Kang, J.S. Kim and J.D. Song analyzed Growth mechanism and TEM results. M. Baik and J. Kyhm wrote the draft. All authors discussed the results and commented on the manuscript.

Funding Sources

Notes

The authors declare no competing financial interest.

Acknowledgements

This research was supported from the IITP grant in KIST funded by the Korea government (MSIT No. 20190004340011001). Also, the research was partially supported from National Research Foundation of Korea (NRF) grant funded by the Korea government (grant No. 2018R1A2A1A05023214, MSIP), an Industry-Academy joint research program between Samsung Electronics - Yonsei University, Basic Science Research Program through the National Research Foundation of Korea(NRF) funded by the Ministry of Education(2016R1A6A1A03012877) and the Korea government(MSIT) (NRF- NRF-2019R1I1A1A01060334).

References

1. Mourad, C., Gianardi, D., and Kapsi, R., 2μm GaInAsSb/AlGaAsSb midinfrared laser grown digitally on GaSb by modulated-molecular beam epitaxy, *Appl. Phys*. **88**, 5543 (2000).
2. Shterengas, L., Kaspi R., Ongstad A. P., Suchalkin, S., and Belenky, G., Carrier capture in InGaAsSb/InAs/InGaSb type-II laser heterostructures, *Phys. Lett.***91**, 101106 (2007)
3. Liao, Y. -A., Hsu, W. -T., Chiu, P. -C., Chyi, J. -I., and Chan, W. -H., Effects of thermal annealing on the emission properties of type-II InAs/GaAsSb quantum dots, *Phys. Lett.***94**, 053101 (2009)
4. Madureira, J. R., De Godoy, M. P. F., Brasil, M. J. S. P., and Iikawa, F., Spatially indirect excitons in type-II quantum dots, *Phys. Lett.***90**, 212105 (2007)
5. Gurioli, M., Wang, Z., Rastelli, A., Kuroda, T. and Sanguinetti, S., Droplet epitaxy of semiconductor nanostructures for quantum photonic devices, *Mater.* **18**, 799–810 (2019)
6. Maimon, S., Finkman, E., and Bahir, G., Inter-sublevel transitions in InAs/GaAs quantum dots infrared photodetectors, *Phys. Lett.* **73**, 2003 (1998)

7. Kirstaedter, N., Schmidt, O. G., Ledentsov, N. N., and Bimberg, D., Gain and differential gain of single layer InAs/GaAs quantum dot injection lasers, *Phys. Lett.* **69**, 1226 (1996)
8. Phillips, J., Bhattacharya, P., Kennerly, S. W., Beekman, D. W., Dutta, M., Self-assembled InAs-GaAs quantum-dot intersubband detectors, *Journal of Quantum Electronics IEEE*, **35**, 6 (1999)
9. Seguin, R., Schliwa, A., Rpdt, S., Potschke, K., Pohl, U. W., and Bimberg, D., Size-Dependent Fine-Structure Splitting in Self-Organized InAs/GaAs Quantum Dots, *Rev. Lett.* **95**, 257402 (2005)
10. Heitz, R., Grundmann, M., Ledentsov, N. N., Eckey, L., Veit, M., and Bimberg, D., Multiphonon-relaxation processes in self-organized InAs/GaAs quantum dots, *Phys. Lett.* **68**, 361 (1996)
11. Fry, P. W., Itskevich, I. E., Mowbray, D. J., Skolnick, M. S., Finley, J. J., Barker, J. A., O'Reilly, E. P., Wilson, L. R., Larkin, I. A., Maksym, P. A., Hopkinson, M., Al-Khafaji, M., David, J. P. R., Cullis, A. G., Hill, G., and Clark, J. C., Inverted Electron-Hole Alignment in InAs-GaAs Self-Assembled Quantum Dots, *Rev. Lett.* **84**, 733 (2000)
12. Takamizu, D., Nishimoto, Y., Akasaka, S., Yuji, H., Nakahara, K., Onuma, T., Tanabe, T., Takasu, H., Kawasaki, M., and Chichibu, S. F., Direct correlation between the internal quantum efficiency and photoluminescence lifetime in undoped ZnO epilayers grown on Zn-polar ZnO substrates by plasma-assisted molecular beam epitaxy, *Appl. Phys*, **103**, 063502 (2008)
13. Chomette, A., Deveaud, B., Clerot, F., Lambert, B., Regreny, A., Optical properties of short-period GaAs/AlGaAs superlattices, *Journal of Luminescence*, vol. 44, **Issues 4-6**, 265-276 (1989)
14. Lambert, B., Deveaud, B., Chomette, A., Regreny, A., and Sermage, B., Density-dependent transition from electron to ambipolar vertical transport in short-period GaAs-AlGaAs superlattices, *Sci. and Tech.*, **Vol. 4**, 7 (1989)
15. Chomette, A., Deveaud, B., Lambert, B., Clerot, F., Regreny, A., Optical detection of vertical transport in short-period GaAs/AlGaAs superlattices, *Superlattices and Microstructures*, **5**, 3, 403-410 (1989)
16. Sun, C.-K., Wang, G., Bowers, J. E., Brar, B., Blank, H.-R., Kroemer, H., and Pilkuhn, M. H., Optical investigations of the dynamic behavior of GaSb/GaAs quantum dots, *Phys. Lett.* **68**, 1543 (1996)
17. Hatami, F., Ledentsov, N. N., Grundmann, M., Bohrer, J., Heinrichsdorff, F., Beer, M., Bimberg, D., Ruvimov, S. S., Werner, P., Gosele, U., Heydenreich, J., Richter, U., Ivanov, S. V., Meltser, Ya., Kop'ev, P. S., and Alferov, Zh. I., Radiative recombination in type-II GaSb/GaAs quantum dots, *Appl. Phys. Lett.* **67**, 656 (1995)
18. Hatami, F., Grundmann, M., Ledenstov, N. N., Heinrichsdorff, F., Heitz, R., Bohrer, J., Bimberg, D., Ruvimov, S. S., Werner, P., Ustinov, V. M., Kop'ev, P. S., and Alferov, Zh. I., Carrier dynamics in type-II GaSb/GaAs quantum dots, *Rev. B,* **57**, 4635 (1998)
19. Suzuki, K., Hogg, R. A., and Arakawa, Y., Structural and optical properties of type II GaSb/GaAs self-assembled quantum dots grown by molecular beam epitaxy, *Appl. Phys.***85**, 8349 (1999)
20. Balakrishnan, G., Tatebayash, T., Khoshakhlagh, A., Huang, S. H., Jallipalli, A., Dawson, L. R., and Huffaker, D. L., III/V ratio based selectivity between strained Stranski-Krastanov and strain-free GaSb quantum dots on GaAs, *Phys. Lett.***89**, 161104 (2006)

21. Weng, X., Burke, R. A., Dickey, E. C., Redwing, J. M., Effect of reactor pressure on catalyst composition and growth of GaSb nanowires, *Cryst. Growth,***312**, 514-519 (2010)
22. Kang, S. S., Park, S. I., Shin, S. H., Shim, C-H., Choi, S-H., and Song, J. D., High-Quality 100 nm Thick InSb Films Grown on GaAs(001) Substrates with an InxAl1−xSb Continuously Graded Buffer Layer, *ACS omega*, **3**, 14562-14566 (2018)
23. Kim, H., and Song, J. D., *Surf. Sci.*, Optical studies on a single GaAs laterally coupled quantum dot incomparison with an uncoupled quantum dot, **Vol. 427**, B, 405-409 (2018)
24. Thibado, P. M., Bennett, B. R., Twigg, M. E., Shanabrook, B. V., and Whitman, L. J., Evolution of GaSb epitaxy on GaAs(001)-c(4×4), *Vac. Sci. Technol. A,* **14**, 885 (1996)
25. Kushwaha, M. S., Lattice Dynamics of ZnS, GaAs, and GaSb, *Stat. Sol. (b)* **98**, 623 (1980)
26. Neuhold, G., Horn,, Zincblende–CdSe on GaSb(110): Characterization of epitaxial growth and electronic structure, *J. Vac. Sci. Technol. A*, **13**, 666 (1995)
27. Gradkowski, K., Pavarelli, N., Ochalski, T. J., Williams, D. P., Tatebayashi, J., Huyet, G., O'Reilly, E. P., and Huffaker, D. L., Complex emission dynamics of type-II GaSb/GaAs quantum dots, *Phys. Lett.* **95**, 061102 (2009)
28. Sun, C.-K., Wang, G., Bowers, J. E., Brar, B., Blank, H.-R., Kroemer, H., and Pilkuhn, M. H., Optical investigations of the dynamic behavior of GaSb/GaAs quantum dots, *Phys. Lett.* **68**, 1543 (1996)
29. Muller-Kirsch,, Pohl, U. W., Heitz, R., Kirmse, H., Neumann, W., and Bimberg, D., Thin GaSb insertions and quantum dot formation in GaAs by MOCVD, *J. Cryst. Growth***221**, 611 (2000)
30. Mahalingam, K., Haugan, H. J., Brown, G. J., Eyink, G., Quantitative analysis of interfacial strain in InAs/GaSb superlattices by aberration-corrected HRTEM and HAADF-STEM, *Ultramicroscopy,* **127**, 70–75 (2013)
31. Sun, C. -K., Wang, G., Bowers, J. E., Brar, B., Blank, H. -R., Kroemer, H., and Pilkuhn, M. H., Optical investigations of the dynamic behavior of GaSb/GaAs quantum dots, *Phys. Lett.***68**, 1543 (1996)
32. Hayne, M., Maes, J., Bersier, S., Moshchalkov, V. V., Schliwa, A., Müller-Kirsch, L., Kapteyn, C., Heitz, R., and Bimberg, D., Electron localization by self-assembled GaSb/GaAs quantum dots, *Phys. Lett.* **82**, 4355 (2003)
33. Gradkowski, K., Ochalski, T. J., Williams, D. P., Healy, S. B., Tatebayashi, J., Balakrishnan, G., O'Reilly, E. P., Huyet. G., and D. L. Huffaker, Coulomb effects in type-II Ga(As)Sb quantum dots, *Status Solidi B,***246**, 752 (2009)
34. Hayne, M., Maes, J., Bersier. S., Moshchalkov. V. V., Schliwa, A., Müller-Kirsch, L., Kapteyn, C., Heitz, R., and Bimberg, D., Electron localization by self-assembled GaSb/GaAs quantum dots, *Phys. Lett.* **82**, 4355 (2003)
35. Jeong, S. Y., Kyhm, J. H., Cha, S. K., Hwang, D. K., Ju, B. K., Park, J. S., Kang, S. J., Han, I.K., High-Speed Colloidal Quantum Dot Photodiodes via Accelerating Charge Separation at Metal–Oxide Interface, *Small*, **201900008** (2019)

36. Libby, W.F., THEORY OE ELECTRON EXCHANGE REACTIONS IN AQUEOUS SOLUTION, *Phys. Chem.* **56**, 863 (1952)
37. Marcus, R. A., Electrostatic Free Energy and Other Properties of States Having Nonequilibrium Polarization. I, *Chem. Phys*. **24**, 979 (1956)
38. Marcus, R. A.,On the Theory of Oxidation-Reduction Reactions Involving Electron Transfer. I, *Chem. Phys.* **24**, 966 (1956)
39. Tang, M., Chen, S., Wu, J., Jiang, Q., Dorogan, V. G., Benamara, M., Mazur, Y. I., Salamo, G. J., Seeds, A., and Liu, H., 1.3-μm InAs/GaAs quantum-dot lasers monolithically grown on Si substrates using InAlAs/GaAs dislocation filter layers, *Express*, **22(10)** 11528-11535 (2014)
40. Kalyuzhnyy, N. A., Mintairov, S. A., Salii, R. A., Nadtochiy, A. M., Payusov, A. S., Brunkov, P. N., Nevedomsky, V. N., Shvarts, M. Z., Martí, A., Andreev, V. M., and Luque, A., Increasing the quantum efficiency of InAs/GaAs QD arrays for solar cells grown by MOVPE without using strain-balance technology, *Photovolt: Res. Appl.*, **24**, 1261-1271 (2016)
41. Suzuki, K. and Arakawa, Y., Growth of stacked GaSb/GaAs self-assembled quantum dots by molecular beam epitaxy, *Cryst. Growth***201**, 1205 (1999)
42. Huang, S. H., Balakrishnan, G., Khoshakhlagh, A., Jallipalli, A., Dawson, L. R., and Huffaker, D. L., Strain relief by periodic misfit arrays for low defect density GaSb on GaAs, *Phys. Lett.*, **88**, 131911 (2006)

Tables

Table 1. Fitting parameters of time resolved PL data at each energy

Energy (eV)	A_1	τ_1 (ns)	A_2	τ_2 (ns)	Average life time(ns)	Charge transfer rate
1.291	29114	0.468	10386.2	3.081	2.300663	3.54721E+08
1.24	28037	0.863	9521.1	4.142	2.895174	2.65466E+08
1.127	7134	1.264	11265.1	5.979	5.422287	1.04488E+08
1.033	887	1.687	4745	8.454	8.21065	4.18570E+07
0.992	0	0	2556.9	11.248	11.248	8.96864E+06
0.953	0	0	1037.2	12.510	12.51 (t_{QD})	0

Figures

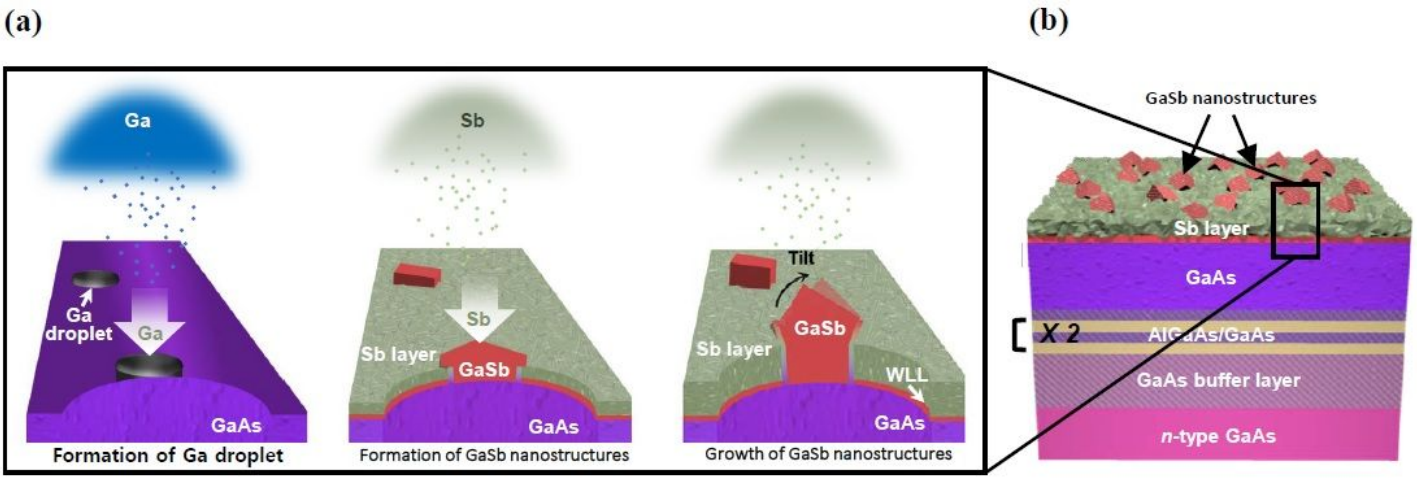

Figure 1

Schematic of (a) self-growth mechanism of the GaSbQD using Ga droplet without GaAs capping layer, and (b) GaSbQD structure on GaAs wafer

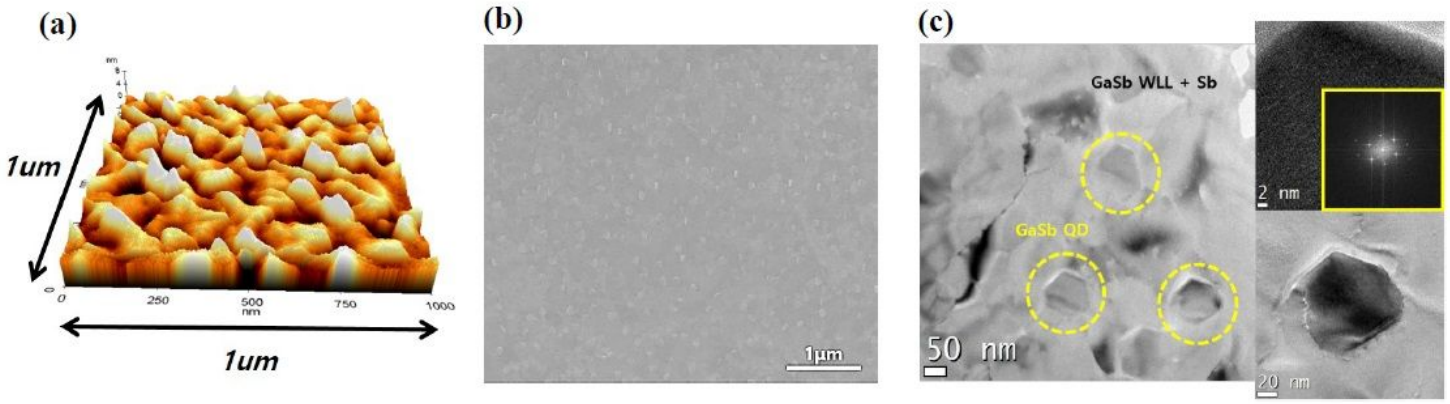

Figure 2

(a) AFM, (b) top-view SEM, and (c) TEM images of self-grown GaSbQD sample without the GaAs capping layer to confirm the density of GaSbQD and shape of the QD

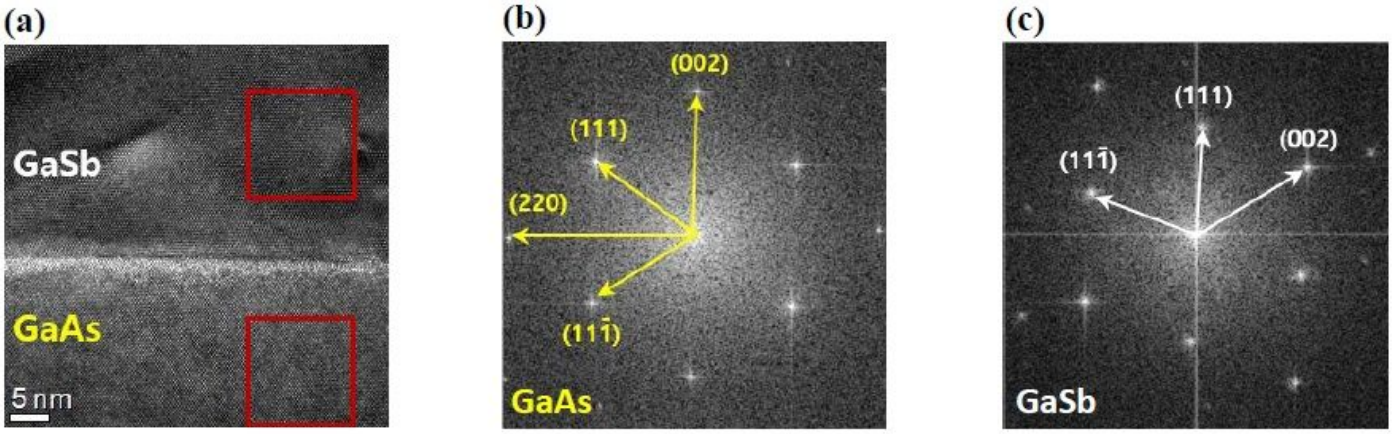

Figure 3

(a) Cross-sectional TEM images of the GaSbQD & GaAs layer, and selected-area diffraction pattern of (b) GaAs layer and (c) GaSbQD for confirming change of growth direction in GaSbQD

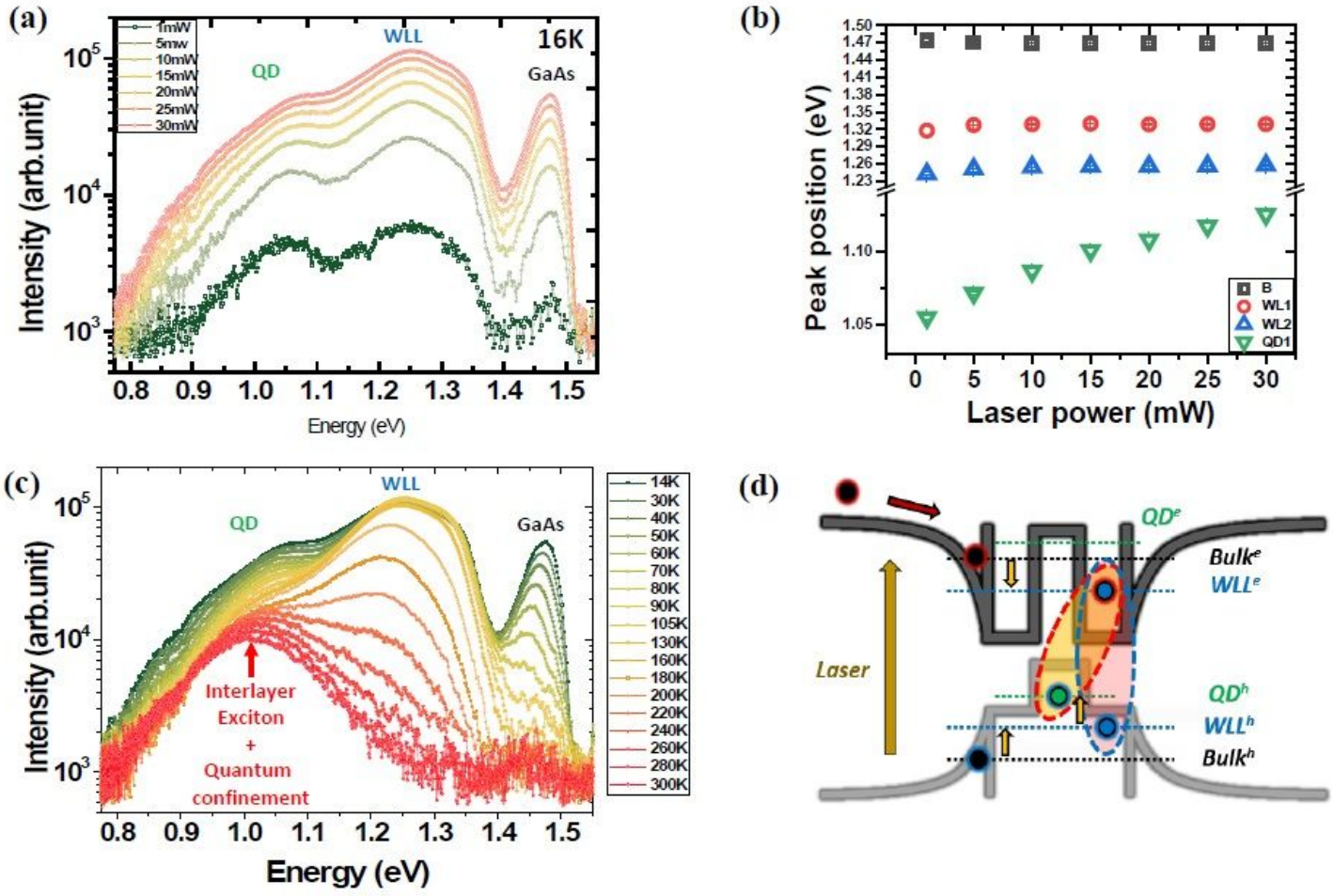

Figure 4

(a) Power-dependent PL spectra at 16 K, (b) each peak energy shift data from laser power of 1 mW to 30 mW, (c) temperature-dependent PL spectra from 14 K to 300 K, and (d) scheme of relaxation processes in self-aligned type-II junction GaSb QD with GaAs capping layer

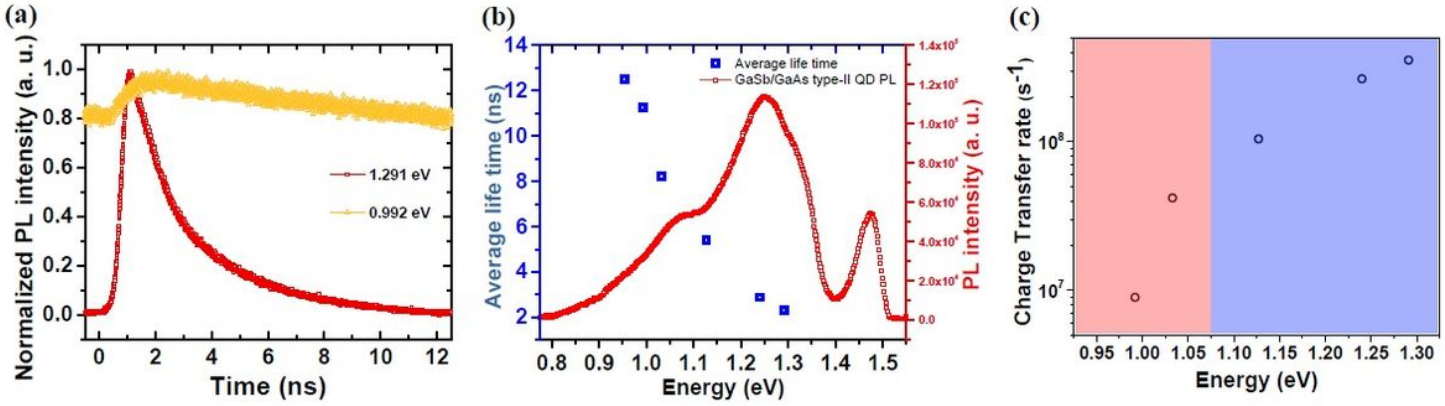

Figure 5

(a) Time-resolved PL spectra at 300 K and (b) average-life time fitting data based on TRPL (c) Many-state Marcus model fitting data of GaSb QD from 0.75 eV to 1.55 eV

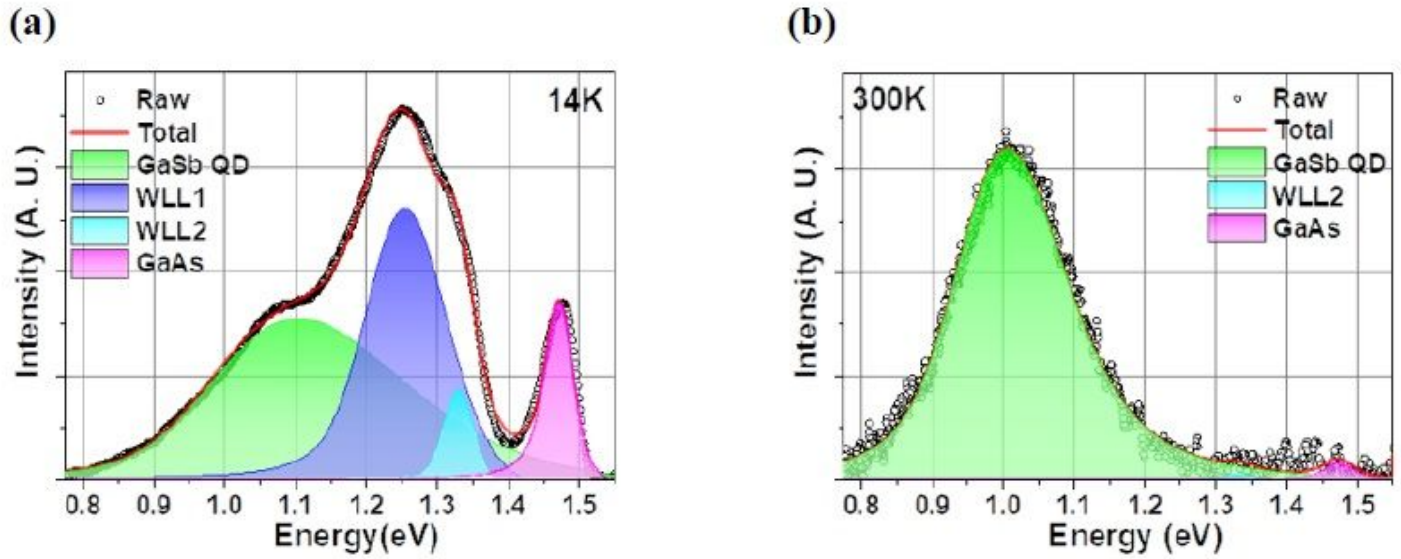

Figure 6

Fitting data of linear scale PL spectra at (a) 14 K and (b) 300 K for calculating Equivalent internal quantum efficiency based on comparing two area of GaSb QD

Supplementary Files

This is a list of supplementary files associated with this preprint. Click to download.

- supportingm.baikGaSbQDfullpaperSCIENTIFICREPORTS.docx